 doi:10.20944/preprints202107.0071.v1

*Article*

# N-Glycomics of human erythrocytes

**Rosaria Ornella Bua [1,2]*, Angela Messina [1], Luisa Sturiale [1], Rita Barone [3], Domenico Garozzo [1], and Angelo Palmigiano [1,]***

[1] CNR, Institute for Polymers, Composites and Biomaterials, (IPCB) Catania, Italy; angela.messina@cnr.it (A.M); luisella.sturiale@cnr.it (L.S); domenico.garozzo@cnr.it (D.G.); angelo.palmigiano@cnr.it (A.P.)
[2] Present address: Laboratorio di Sanità Pubblica, sezione Tossicologia, Azienda Sanitaria Provinciale (ASP), Catania, Italy; ornella.bua87@gmail.com (R.O.B.)
[3] Child Neurology and Psychiatry, Department of Clinical and Experimental Medicine, University of Catania, Catania, Italy; rbarone@unict.it (R.B.)
* Correspondence: angelo.palmigiano@cnr.it (A.P.); ornella.bua87@gmail.com (R.O.B); Tel.: +39-0957338250 (A.P.)
* These authors have contributed equally to this work.

**Abstract:** Glycosylation is a complex post-translational modification that conveys functional diversity to glycoconjugates. Cell surface glycosylation mediates several biological activities such as induction of intracellular signaling pathway and pathogen recognition. Red blood cell (RBC) membrane N-glycans determine blood type and influence cell lifespan. Although several proteomic studies were carried out, glycosylation of RBC membrane proteins has not been systematically investigated. This work aims at exploring the human RBC N-glycome by high-sensitivity MALDI-MS techniques to outline a fingerprint of RBC N-glycans. To this purpose, MALDI-TOF spectra of healthy subjects harboring different blood groups were acquired. Results showed the predominant occurrence of neutral and sialylated complex N-glycans with bisected N-acetylglucosamine, core- and/or antennary fucosylation. In the higher mass region these species presented with multiple N-acetyllactosamine repeating units. Amongst the detected glycoforms, the presence of glycans bearing ABO(H) antigens allowed us to define a distinctive spectrum for each blood group. For the first time, advanced glycomic techniques have been applied to a comprehensive exploration of human RBC N-glycosylation, providing a new tool for the early detection of distinct glycome changes associated with disease conditions as well as to understand pathogens molecular recognition.

**Keywords:** Red Blood Cells, N-glycosylation, MALDI-TOF, ABO(H) blood groups

## 1. Introduction

The Red blood cell (RBC), or erythrocyte, is the simplest human cell as it does not have internal organelles, lost during the erythropoiesis process. RBCs develop in the bone marrow and have a life span of about 100–120 days before they are recycled by macrophages [1]. In the last decade, several studies were carried out to shed light on the biological function of RBC membrane proteins [2,3]. As a result, the erythrocyte membrane is one of the best-known membranes in terms of structure, function, and associated genetic disorders [4–6]. RBC membrane mediates transport functions and provides the erythrocytes with their structural features of resilience and deformability [7].

Glycosylation is a post-translational modification characterized by the covalent linkage of oligosaccharides moieties (glycans) to form glycoconjugates. Glycans are conjugated to asparagine (N-glycan) or serine/threonine (O-glycans) residues to form glycoproteins. Protein glycans play important roles in biological function/activity, protein folding and molecular recognition [8]. Glycans are also recognized by glycan-proteins with lectin activity on opposing cells and these glycan-ligand interactions are responsible

Preprints (www.preprints.org) | NOT PEER-REVIEWED | Posted: 2 July 2021 doi:10.20944/preprints202107.0071.v1

for many biological activities, including induction of intracellular signaling pathway and recognition of pathogens such as influenza virus [8,9].

Changes in N-linked glycosylation have long been associated with disease development and acquired glycan modifications have been described in multifactorial diseases such as cancer [10,11], inflammation [12,13], neurodegeneration [14,15] and genetic diseases [16,17].

Human RBC protein glycosylation has not been systematically examined in its entirety as yet [18], though previous studies investigated the two most abundant glycoproteins of the erythrocyte membrane, namely band 3 and glycophorin A (GPA) [19-22]. In human erythrocytes, band 3 and other red blood cell membrane proteins bear poly-N-acetyllactosamine (poly-LacNAc) extensions, acting as antigen carrier during various stages of cell development and differentiation [18,19]. The ABO(H) antigens were found as terminal non-reducing epitopes of large complex RBC N-glycans [23,24], and also constitute distinctive traits of outer arm glycophorin N-linked structures at lower molecular masses [18,25]. They play crucial roles in transfusion medicine, determining the compatibility between blood donors and recipients, as well as in the development of several hemostasis-related genetic disorders, including cardiovascular diseases and thrombosis [26,27]. Futhermore, several studies have investigated the relationship between the ABO(H) blood group distribution and the occurrence of some infectious diseases, such as HIV, malaria, influenza [28-33] and, recently, COVID-19 pandemic [34-37].

Although information on the biological roles of glycan-binding proteins is still rising, challenges remain in detecting and profiling known and novel cellular glycans structures, due to the vast heterogeneity of possible glycoprotein isoforms depending on glycan occupancy of protein glycosylation sites (macroheterogeneity), and on the variety of the attached glycans (microheterogeneity). Macroheterogeneity is related to the site availability, enzyme kinetics, and substrate concentrations that regulate the N-glycan precursor assembly and its subsequent transfer to the protein in cytosol and endoplasmic reticulum, whereas microheterogeneity is associated to N-glycan processing occurring in endoplasmic reticulum and Golgi [17]. In this context, mass spectrometry (MS) techniques have demonstrated their capability for characterization of unknown glycans and high-throughput analysis of known glycan structures, allowing to distinguish individual glycoforms [38]. Advances in mass spectrometry, and in particular in matrix-assisted laser desorption/ionization time-of-flight (MALDI-TOF) MS, have driven glycan analysis to substantial progresses [39]. The eligibility of MALDI-TOF is established because of its ability to analyze complex mixtures of glycans from biological samples together with its high detection sensitivity, as exemplified by several glycomic studies [40-42].

Since RBCs are continuously replenished with glycosylated membrane proteins that can be isolated, purified and readily available from blood samples, glycosylation analysis of erythrocyte membrane glycoproteins might be the key for the early detection of glyco-biomarkers for diagnostic and therapeutic purposes as well as for studying interaction mechanisms involved in recognition of pathogens. In the present study, we applied high-sensitivity MALDI TOF MS-based glycomic methodologies to the analysis of total N-glycans derived from human erythrocyte membrane proteins, with the aim to generate a N-glycosylation fingerprinting of RBC. In particular, the total N-glycome of healthy subjects with different ABO(H) blood groups is evaluated as the starting point for future investigations.

## 2. Results

### *2.1. RCB N-glycoprofiles by MALDI-MS*

Preprints (www.preprints.org) | NOT PEER-REVIEWED | Posted: 2 July 2021 doi:10.20944/preprints202107.0071.v1

Representative N-glycan profiles of membrane glycoproteins from human erythrocyte (blood groups A, B, AB and O) are reported in Figure 1A-D and in Supplementary Figures 1-12. Each MALDI mass spectrum is very dense of peaks, showing some hundreds of assigned glycoforms which correspond to a wide range of N-Glycan categories, including a full complement of oligomannose structures and series of complex glycans, mainly with bisecting N- acetylglucosamine (GlcNAc), as well as neutral, acidic, and hybrid species. All the acquired mass spectra were found very similar, with the distinguishing factor being the blood group epitope-bearing structures. In particular, the low mass range of each spectrum (Figure 1A-D) is very informative as it comprises N-glycans structures with none, one or both the ABO(H) antigens. Below a detailed description of the main N-glycan families recognized in the RBC N-glycome fingerprinting.

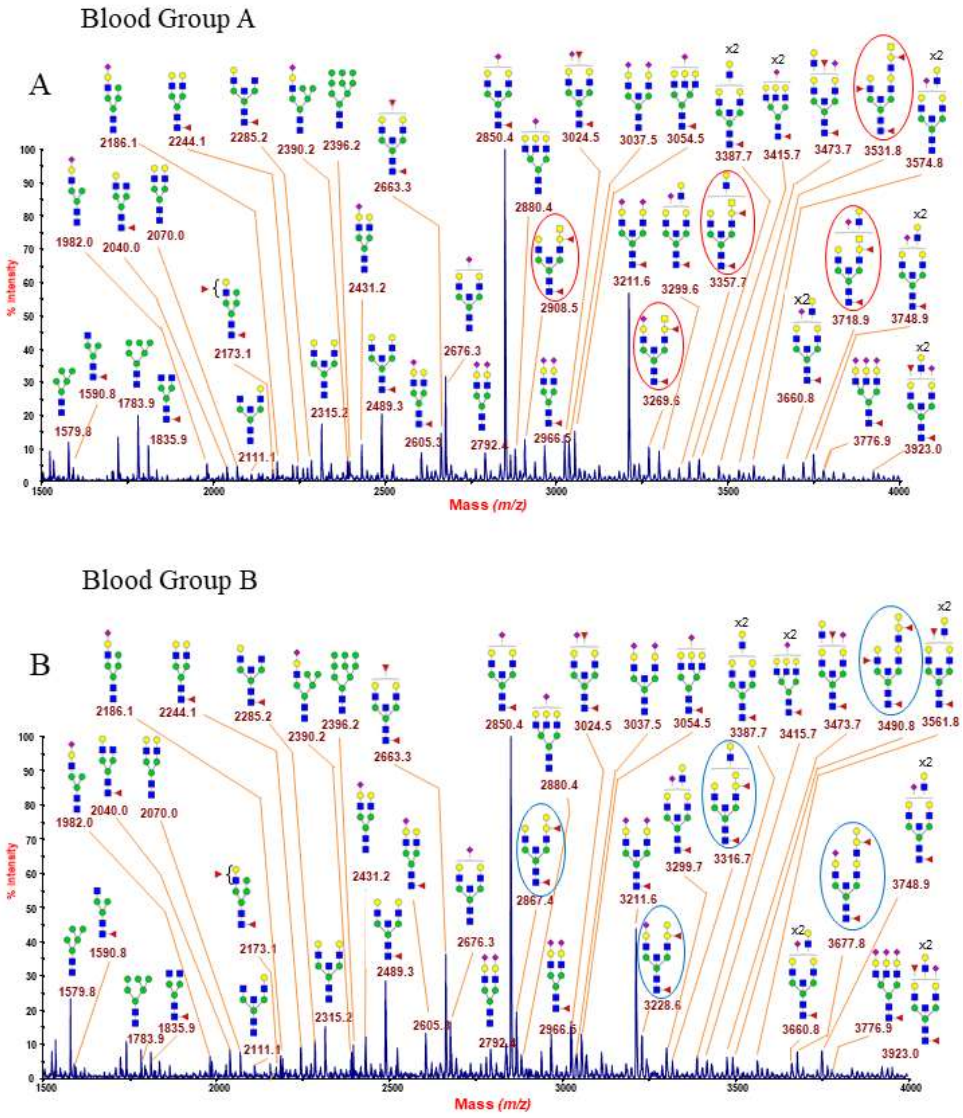


**Figures 1 A-B. MALDI-TOF mass spectra at low mass-range (m/z 1500-4000) showing molecular ions [M+Na]+ of permethylated N-linked glycans from human erythrocytes blood groups A and B.** MALDI-TOF MS mapping of permethylated N-glycans from RBC are distinctive of each blood group. (A) Blood group A, (B) blood group B, Structures consistent with glycoforms comprising blood group A and blood group B epitopes are highlighted with red and blue, respectively. N-acetylglucosamine (GlcNAc), blue square; Mannose (Man), green circle; Galactose (Gal), yellow circle; Sialic acid (NeuAc), purple lozenge; Fucose (Fuc), red triangle.

Preprints (www.preprints.org) | NOT PEER-REVIEWED | Posted: 2 July 2021 doi:10.20944/preprints202107.0071.v1

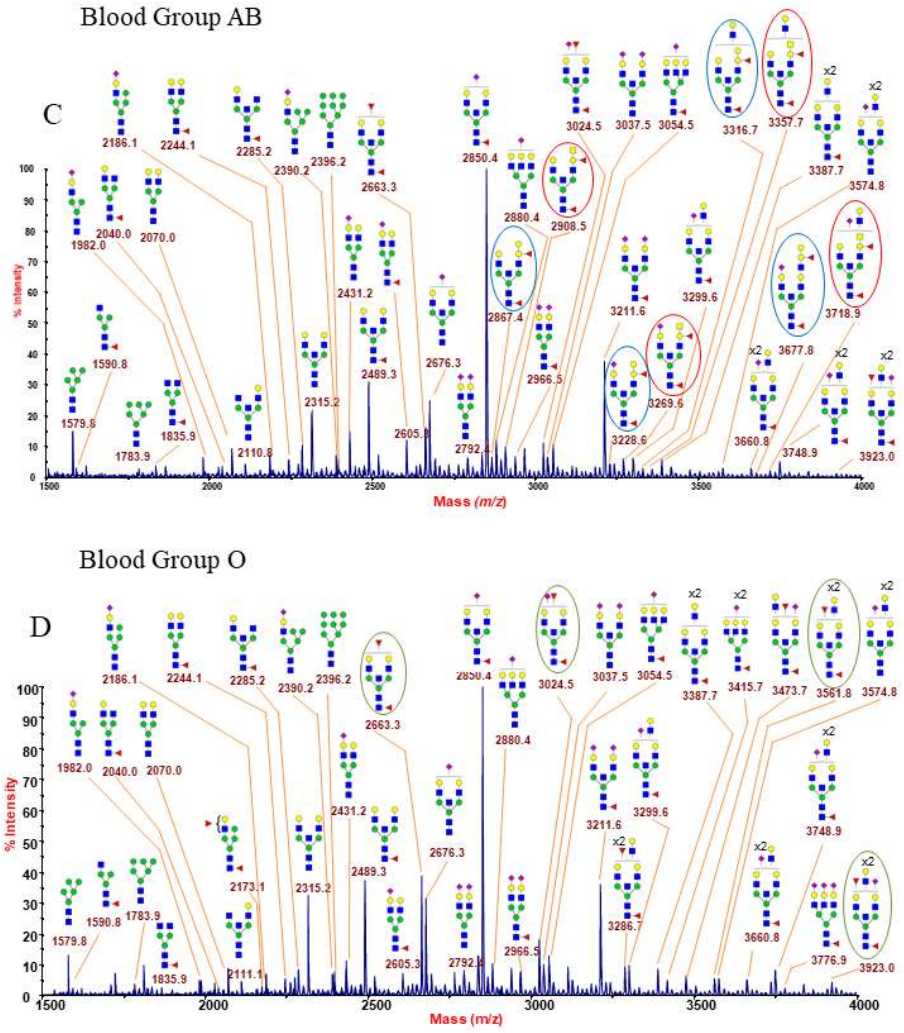


**Figures 1 C-D. MALDI-TOF mass spectra at low mass-range (m/z 1500-4000) showing molecular ions [M+Na]+ of permethylated N-linked glycans from human erythrocytes blood groups AB and O.** MALDI-TOF MS mapping of permethylated N-glycans from RBC are distinctive of each blood group. (C) Blood group AB, and (D) blood group O. Structures consistent with glycoforms comprising blood group A, blood group B and blood group O epitopes are highlighted with red, blue, and green circles, respectively. N-acetylglucosamine (GlcNAc), blue square; Mannose (Man), green circle; Galactose (Gal), yellow circle; Sialic acid (NeuAc), purple lozenge; Fucose (Fuc), red triangle.

### 2.1.1. Oligomannose N-glycans

Oligomannose N-glycans structures were observed at m/z 1579.8 (Man5), 1783.9 (Man6) and 2396.2 (Man9), as reported in Figure 1A-D and in Supplementary Figures 1, 4, 7 and 10.

### 2.1.2. Hybrid N-glycans

Minor amounts of hybrid glycans were also detected at m/z 2173.1, corresponding to structures with core and peripheral fucosylation, and at m/z 2186.1 and 2390.2 attributable to sialylated species (Figure 1A-D and Supplementary figures 1, 4, 7 and 10).

### 2.1.3. Bisected N-glycans

 doi:10.20944/preprints202107.0071.v1

Amongst the N-glycan structures showed in Figure 1A-D and in the Supplementary Figures 1-12, bisected N-glycans were the most abundant species. The main ion peaks, at m/z 2850.4 and 3211.6, corresponded to fucosylated mono and disialo-biantennary oligosaccharides with a bisecting GlcNAc residue, as reported by previous studies [21,22,25]. Bisecting GlcNAc is a common structural feature of erythrocyte N-glycans, together with antennary fucosylation and a significant sialylation level [19-22,25,43,44]. Most of the bisected N-glycans here identified showed core fucosylation and poly-LacNAc branching.

#### 2.1.4. Poly-LacNAc N-glycans

In the middle/high mass regions of the spectra (showed in the respective Supplementary Figures), N-glycans bearing poly-LacNAc extensions (Galβ1-4GlcNAcβ1-3-) were observed, with the largest glycans possessing about a dozen of LacNAc repeats. It is reasonable expected that large structures, with more than two LacNAc extensions, may carry the major portion of ABO(H) antigens as terminal epitopes, producing a very complex typical fingerprint of each blood group.

#### 2.1.5. Sialylated N-glycans

In our MALDI MS spectra, sialylation was as a relatively abundant terminal decoration, especially in the higher mass regions with the largest glycans bearing between one and three sialic acid (NeuAc) terminated epitopes on their antennae.

#### 2.1.6. ABO(H) antigen-bearing N-Glycans

Figure 1A reports a typical RBC N-glycan MALDI spectrum for blood group A focused on the mass-range between m/z 1500 and 4000. The related epitope [GalNAcα1-3(Fucα1-2)Galβ1-4GlcNAc-] was found as terminal side chain substitution of the glycoforms at m/z 2908.5, 3269.6, 3357.7, 3531.8, 3718.9, 3806.9 and 3981.0 (Figure 1A and Supplementary Figures 1 and 2), as demonstrated by further in-depth structural characterizations by MALDI TOF/TOF MS/MS. Moreover, over m/z 4000, a number of molecular ions was found consistent with bisected N-glycans bearing poly-LacNac elongations mostly terminating with blood group A antigen or NeuAc, as shown in Supplementary Figures 2 and 3. A great deal of the assigned structures was confirmed by MS/MS analysis. As a representative example, the fragmentation spectrum of the molecular ion at m/z 2908.5 is reported in Figure 2.

Preprints (www.preprints.org) | NOT PEER-REVIEWED | Posted: 2 July 2021 doi:10.20944/preprints202107.0071.v1

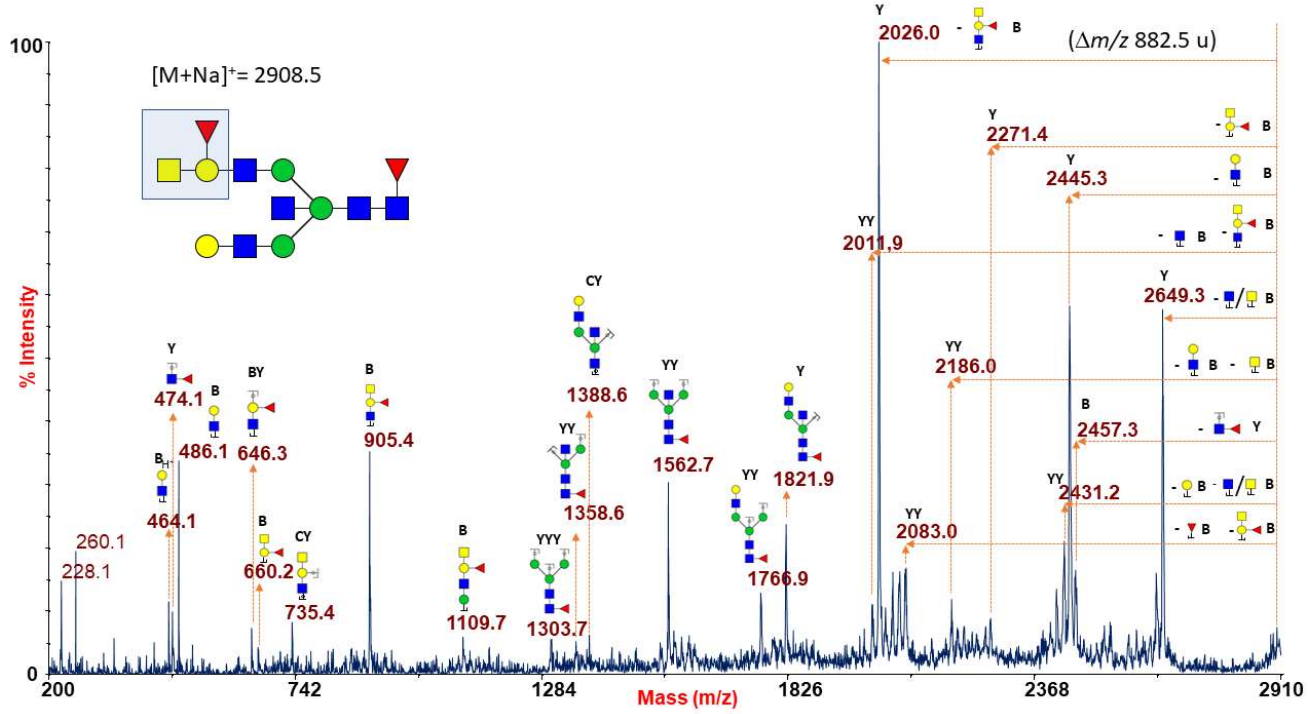


**Figure 2. MALDI TOF/TOF MS/MS characterization of the N-glycan precursor at m/z 2908.5 from blood group A human erythrocytes.** All the fragmentation pattern points to delineate a N-linked glycan moiety with a terminal blood group A epitope (sketched in the reported structure), as mainly revealed by B-type ions at m/z 660.2, 905.4 and 1109.7, by the predominant Y ion at m/z 2026.0 (◎m/z 882.5 u from the parent ion) and by a further Y ion at m/z 2271.4. GlcNAc, blue square; Man, green circle; Gal, yellow circle; NeuAc, purple lozenge; Fuc, red triangle.

It comprises intense B and Y ions originated from glycosidic linkage cleavages, (Domon and Costello nomenclature [45]), mainly present on permethylated glycans fragmentation patterns. In particular, the non-reducing terminal A antigen of the molecular ion at m/z 2908.5 gave rise, in the low mass-range, to a series of B ions at m/z 660.2, 905.4, 1109.7, together with internal fragments at m/z 646.3 (BY ion) and 735.4 (CY ion), eliciting in the high mass-range a very intense Y fragment at m/z 2026.0 due to the blood group A epitope loss from the parent ion.

Likewise, the B antigen [Gal$\alpha$1-3(Fuc$\alpha$1-2)Gal$\beta$1-4GlcNAc-] was found as side chain substitution of the glycoforms at m/z 2867.4, 3228.6, 3316.7, 3490.8,3677.8, 3765.9, and 3940.0 (Figure 1B and Supplementary Figures 4 and 5), and was coherently suggested as terminal structural motif of a number of high-mass glycans up to m/z 8082.0 (see highlighted structures in Supplementary Figures 5 and 6). Figure 3 shows the MS/MS spectrum of a typical B antigen-bearing N-glycan structure, i.e., the ion at m/z 3677.8 present in Figure 1B and Supplementary Figure 5.

Preprints (www.preprints.org) | NOT PEER-REVIEWED | Posted: 2 July 2021 doi:10.20944/preprints202107.0071.v1

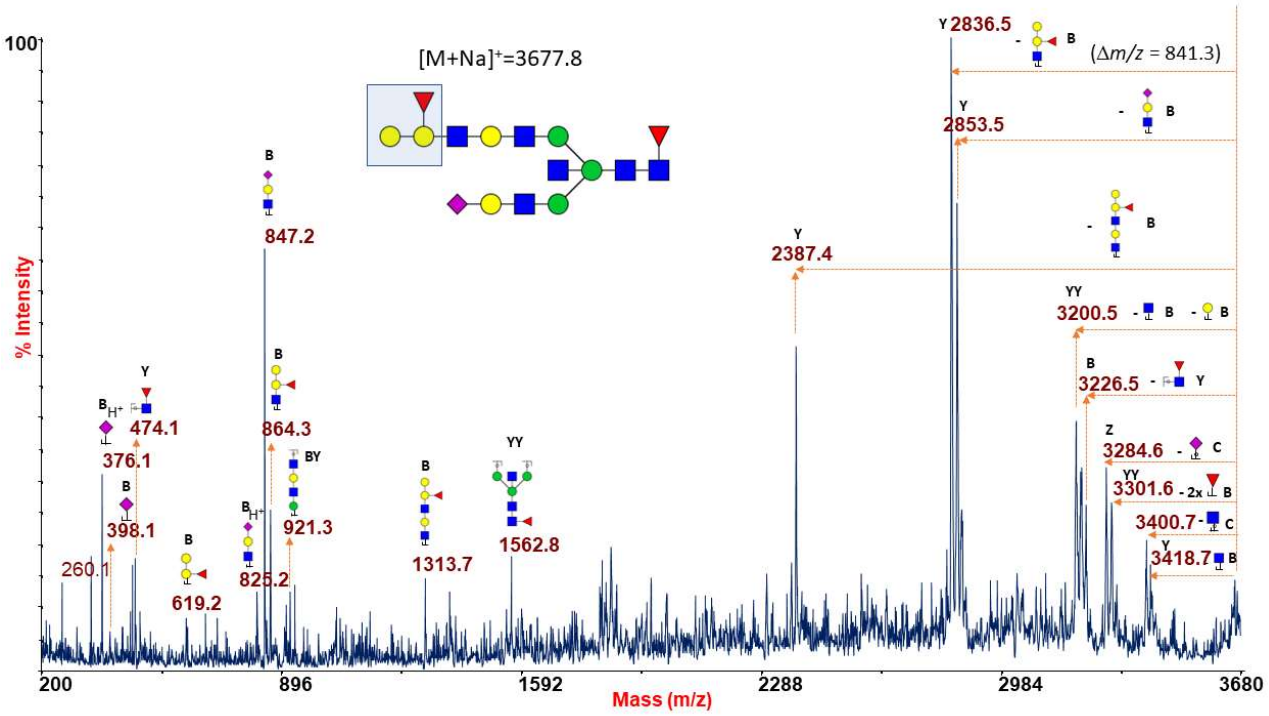


**Figure 3. MALDI TOF/TOF MS/MS characterization of the N-glycan precursor at m/z 3677.8 from blood group B human erythrocytes.** All the fragmentation pattern points to delineate a N-linked glycan moiety with a terminal blood group B epitope (sketched in the reported structure), as mainly revealed by B-type ions at m/z 619.2, 864.3 and 1313.7, by the predominant Y ion at 2836.5 (⌾m/z 841.3 u from the parent ion) and by a further Y ion at m/z 2387.4. GlcNAc, blue square; Man, green circle; Gal, yellow circle; NeuAc, purple lozenge; Fuc, red triangle.

The fragmentation pattern comprised a series of peaks demonstrating the occurrence of a B antigen, as B-type ions at m/z 619.2, 864.3 and 1313.7, the internal fragment at m/z 3200.5 (YY ion), revealing the loss of terminal unsubstituted galactose (Gal) and GlcNAc units, and the intense Y ion at m/z 2836.5 originated from the loss of blood group B epitope from the parent ion.

The RBC N-glycan MS analysis of blood type AB is reported in Figure 1C and in Supplementary Figures 7-9. These spectra comprise both N-glycans carrying A or B antigens, originating couples of peaks with ⌾m/z 41, due to the mass shift between the correspondent permethylated structures bearing group A or Group B epitopes (i.e., m/z 2867.4 and 2908.5, 3228.6 and 3269.6, 3316.7 and 3357.7, 3677.8 and 3718.9 in Figure 1C), also found up to m/z 7761.9 (see Supplementary Figures 8 and 9). As expected, MS/MS analyses of those N-glycans carrying specific antigens in AB group MS profiles, yielded identical results as the respective A and B antigen-bearing ions detected in A or B blood group RBC samples (data not shown).

Figure 1D finally shows the N-glycan MS profile, at low mass-range (m/z 1500-4000), representative of the O (H) blood group RBC. Increased intensity of molecular ions consistent with glycoforms carrying the blood group H epitope (Fuc$\alpha$1-2Gal$\beta$1-4GlcNAc) was observed at m/z 2663.3, 3024.5, 3286.7, 3561.8, 3923.0 (see also Supplementary Figures 10 and 11). Blood group O individuals have functionally inactive A/B glycosyltransferases and therefore their H antigen, the starting substrate for distinctive A/B blood group epitopes, remains unmodified [46]. As a consequence, the whole MS profile (as also reported in Supplementary Figures 11 and 12), is characterized by the lack of antigen-bearing N-glycans with unique molecular masses. MS/MS analyses of the species at m/z 2663.3 and 3923.0, are presented as significant examples. The ion at m/z 2663.3 (Figure 4) gave a fragmentation spectrum characteristic of both core and antennary fucosylation. In particular,

Preprints (www.preprints.org) | NOT PEER-REVIEWED | Posted: 2 July 2021 doi:10.20944/preprints202107.0071.v1

the B/Y ion pairs at m/z 864.4/1821.9 and 660.3/2026.0, together with the internal fragment at 432.2 (H+ form), implying the alternative location of the peripheral fucose either on terminal Gal and on antennary GlcNAc residue, suggested the possible occurrence of either H antigen or Lewis epitope as terminal side-chain substitution.

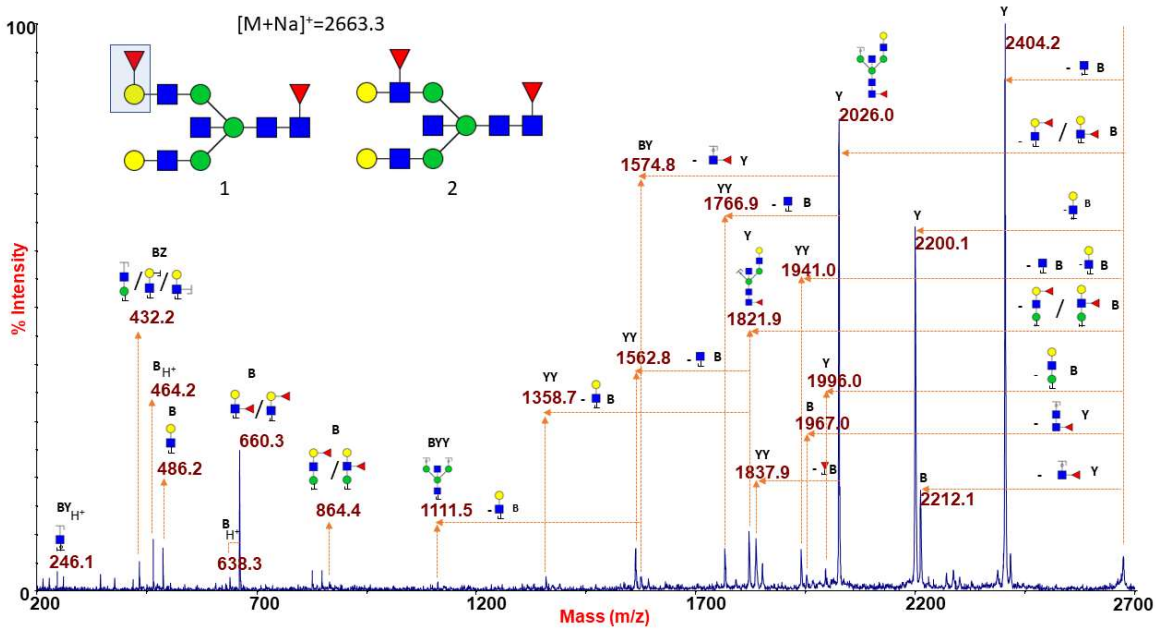


**Figure 4. MALDI TOF/TOF MS/MS characterization of the N-glycan precursor at m/z 2663.3 from blood group O human erythrocytes.** The reported spectrum shows the occurrence of two distinct isomers differing in the position of the antennary fucose. Fragments at m/z 660.3 and 864.4 (B ions) and at m/z 2026.0 and 1821.9 (Y ions) indicated this monosaccharide may be linked either to a terminal Gal, giving rise to a blood group H antigen (as sketched in structure 1), and to an antennary GlcNAc, thus originating a Lewis epitope (structure 2). GlcNAc, blue square; Man, green circle; Gal, yellow circle; NeuAc, purple lozenge; Fuc, red triangle.

Similar results were obtained when analyzing the species at m/z 3923.0, (Figure 5), corresponding to a possible mixture of isobaric species with mono- and tri-LacNAc extensions at the two branches which may be alternatively capped with NeuAc or antigen H/Lewis epitopes. Further fragmentation analyses of molecular ions at m/z 3024.5, 3286.7 and 3561.8 concurred to postulate the co-presence of N-glycan isomers bearing H or Lewis antigens (data not shown).

Preprints (www.preprints.org) | NOT PEER-REVIEWED | Posted: 2 July 2021 doi:10.20944/preprints202107.0071.v1

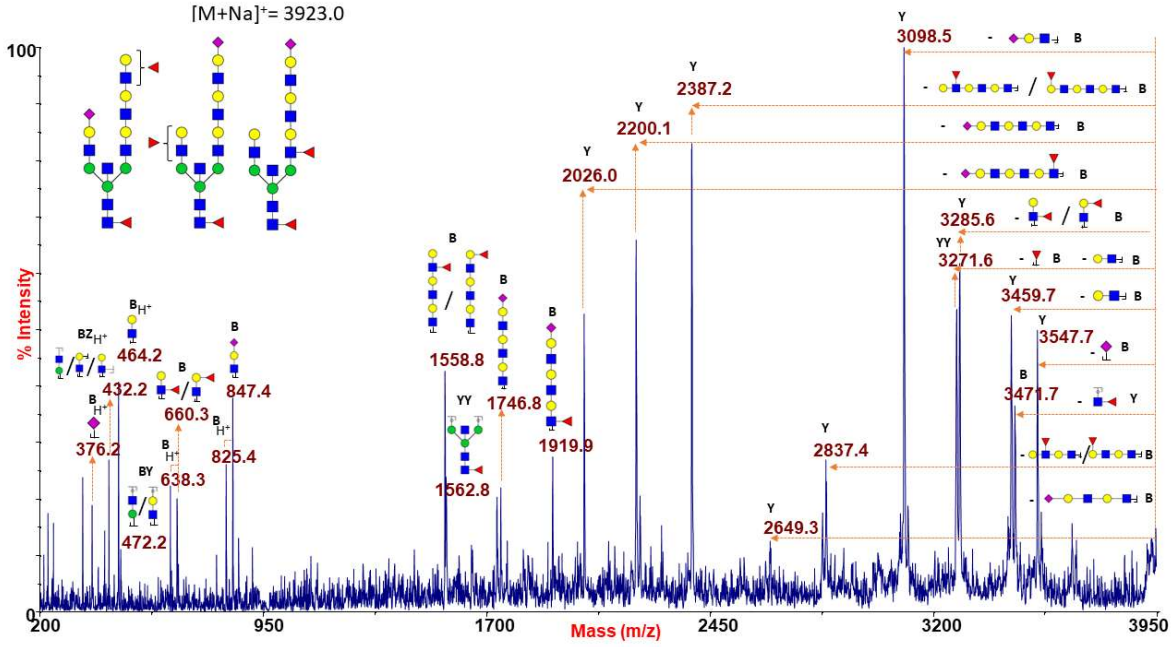


**Figure 5. MALDI TOF/TOF MS/MS analysis of the N-glycan precursor at m/z 3923.0 from blood group O human erythrocytes.** This fragmentation spectrum shows B and Y ion series revealing the co-presence of different isoforms characterized by mono- to tri-LAcNAc extensions which may be terminated with NeuAc or H antigen/Lewis epitopes. GlcNAc, blue square; Man, green circle; Gal, yellow circle; NeuAc, purple lozenge; Fuc, red triangle.

## 3. Discussion

In the present study we applied a robust and widely used MS-based glycomic approach to the extensive N-glycan characterization of RBCs. Our MALDI-TOF data showed erythrocyte membrane glycoproteins holding in prevalence complex bisected N-glycans with core and antennary fucosylation and recurrent poly-LacNAc extensions, in accordance with earlier glycosylation studies on specific red blood cell membrane proteins. Previous characterization of RBCs N-glycoproteins has been limited to their main components, such as band 3 and GPA proteins [19-22,25]. Band 3 was found harboring a single N-linked oligosaccharide, with a branched structure varying in the number of repeating LacNAc units terminated with Gal, fucose (Fuc) or NeuAc [19,20], whereas GPA, a major glycophorin, has been reported to bear fifteen O-glycans [47,48] and a single N-linked glycan, mostly a biantennary sialylated moiety with bisecting GlcNAc and outer arm fucosylation [21,22]. In the current study, MALDI-TOF strategy allowed a broad characterization of the total RBC N-glycans released from band 3, GPA and from additional minor glycoproteins. We observed large N-glycan structures up to 9kDa (see Supplementary Figures) as a result of the ad hoc developed MS strategy that led to a notable improvement in upper mass range sensitivity and signal-to-noise ratio. Besides a predominant portion of complex highly processed structures, we additionally found oligomannose and hybrid N-glycans. As glycan structures are generated in the compartmentalized Golgi, changes in the relative signals of all the observed RBC N-glycans could be used as a diagnostic tool for the detection of defects in glycosylation enzymes involved in early Golgi processing in glycosylation-related diseases [43,49-51]. However, only a few studies reported on the N-glycosylation of human erythrocyte membrane glycoproteins using MS techniques [43,44,52], mostly focusing on the characterization of glycans from band 3 membrane glycoprotein in congenital dyserythropoietic anemia type II (CDA II), also called hereditary erythroblastic multinuclearity with the positive acidified-serum test (HEMPAS) [43,44]. Fukuda et al. in 1987 developed a method based on fast-atom bombardment (FAB) MS [43], whereas Denecke et al. in 2008 [44] compared erythrocyte band 3 mass mapping from

Preprints (www.preprints.org) | NOT PEER-REVIEWED | Posted: 2 July 2021 doi:10.20944/preprints202107.0071.v1

HEMPAS and from control by MALDI-TOF MS following SDS-PAGE and lectin-binding strategies. Both these studies accordingly found the lack of the large oligosaccharide component bearing the poly-LacNAc branches and the prevalence of glycans at lower molecular mass (such as oligomannose, hybrid and truncated complex species) in the red blood cell band 3 glycoprotein from HEMPAS patients, suggesting a defective Golgi processing in erythroblasts [43,44].

RBC membrane N-glycans are particularly exposed to the external environment, supporting the pathogen recognition processes. For instance, the hemagglutination assay is based on the interaction between the hemagglutinin located on the surface of the human-adapted influenza virus and some specific sialylated glycans on the epithelial cells of the human upper respiratory tract, defined as the key initial step of the infection cycle [53]. Accordingly, agglutination of chicken RBCs (cRBCs) [54] has long been used in viral titer assays as well as to investigate glycan receptor binding sites and testing vaccines effectiveness [55-58]. Structural characterization of cell surface N-glycans of cRBCs, revealed the presence of bi- and triantennary structures capped with both $\alpha$2→3 and $\alpha$2→6 linked NeuAc, and the lack of lactosamine repeating units [54]. On the other hand, the human bronchial epithelial cells, which are the target of human-adapted influenza A viruses, show the predominance of $\alpha$2→6 sialylated glycans with lactosamine repeats [59,60]. These data could explain some pitfalls of agglutination assay based on cRBCs which may not be representative of the physiological receptor for human-adapted influenza strains. Our study may trigger future advanced MS-based structural analyses on glycans from human RBCs, providing important insights for improved applications in this field.

The applied MALDI-TOF MS and MS/MS strategy here presented, allowed to well characterize glycans bearing the ABO(H) blood group antigens which, like genetic factors, are involved in several hemostasis-related diseases [26,27] and in many infectious diseases [28-33]. Several shreds of evidence suggest that the ABO(H) blood group expression may influence the development and the progression of cardiovascular disease, thrombosis, and hemostasis disorders. In the last year, there has been a growing interest in studying the association between the ABO(H) blood group distribution and the dynamics of COVID-19 pandemic [34-37]. Recently, Liu et al. [36] found a positive correlation between the occurrence of COVID-19 infection cases and the proportion of blood group A by analysing the data from the official WHO database. These results agree with other previous studies [34,35], strongly suggesting a relationship between the distribution of blood groups and the SARS-CoV-2 infection. However, the underlying mechanisms have not yet been clarified and further investigation, also taking into account the glycan-binding specificity and the SARS-CoV-2 proteins glycosylation features, are highly needed.

## 4. Materials and Methods

### *4.1. Erythrocyte Isolation*

Peripheral whole blood samples in anticoaugulant tubes were obtained from healthy subjects which underwent blood type analyses. Procedures were performed according to Helsinki declaration after obtaining written informed consents from all participants. The erythrocytes were isolated by centrifugation for 10 min at 4000 rpm. The supernatant, composed of plasma and buffy coat (leukocyte and platelets), was removed and the cell pellet was washed three times with 3 ml of 0.9% saline solution.

### *4.2. Hemolysis and extraction of membrane proteins*

Erythrocyte membranes were prepared by slightly modifications of a previously reported protocol [61]. Erythrocytes (500 µL) were suspended in an equal volume of saline solution and as such constituted the erythrocyte suspension. Hemolysis was performed by adding 10 volumes of ice-cold hypotonic phosphate buffer (1.43 mM NaH2PO4, 5.7 mM Na2HPO4, pH 7.4). This mixture was gently stirred for 45 min at 4 °C and the

 doi:10.20944/preprints202107.0071.v1

membranes were settled by centrifugation for 12 min at 12000 rpm. The supernatant was carefully removed, and the pellet was washed 5-6 times with 10 volumes of hypotonic phosphate buffer till a white ghost appeared. Then, the supernatant was removed, and the ghosts were lyophilized. RBC membrane glycoproteins extractions were performed by RapigestTM surfactant (Waters Corporation, Milford, Massachusetts) as a denaturing agent. About 5 mg of erythrocyte membranes were resuspended in 220 µL of RapigestTM 0.1% in 50 mM bicarbonate buffer and the obtained mixture were boiled at 100 °C for 7 minutes. After cooling, samples were reduced in 5 mM dithiothreitol (DTT, Sigma) at 56°C for 30 min and alkylated in 15 mM iodoacetamide (IAA, Sigma) in the dark at room temperature for 30 min. The N-linked glycans were released by 4 U of peptide N-glycosidase F (PNGase F, EC 3.5.1.52; Roche Diagnostics GmbH) digestion at 37°C overnight. The enzymatic digestions were stopped by adding HCl (to a final concentration of 40 mM, pH ≤ 2) and incubated at 37°C for 45 min. After dilution with MilliQ water to a final volume of 1 mL, samples were centrifuged 10 min at 13000 rpm and the unsolved material was removed. The obtained N-glycans were purified by 3 cc C18 Sep-Pak cartridges (Waters Milford MA), followed by a further purification step by solid-phase extraction (SPE) (Hypersep Hypercarb, Thermo Fisher Scientific Inc.), and finally permethylated as detailed described previously [62,63], to enhance mass spectrometric detection sensitivity.

### *4.3 MALDI TOF MS and MS/MS analysis*

A few microliters of permethylated N-glycan samples, resuspended in methanol, were mixed with the same volume of matrix solution (10 mg/ml 5-Chloro-2-mercaptobenzothiazole, CMBT in MeOH/H2O 80/20). MALDI TOF and MALDI TOF/TOF mass spectra were recorded in reflectron mode and positive polarity using a 4800 MALDI TOF/TOF™ (Applied Biosystems) instrument, equipped with an Nd:YAG laser at 355-nm and 200 Hz repetition rate. In MS mode, 1200 shots were accumulated for each spectrum, with a resolution greater than 15K and a mass accuracy better than 75 ppm. A 4700-calibration standard kit, calmix (Applied Biosystems) was used as external calibrant for the MS mode, and [Glu1] fibrinopeptide B human (Sigma) was used as external calibrant for the MS/MS mode (1 µL of TOF/TOF Calibration Mixture in 24 µL of CHCA matrix solution).

### *4.4. Data Evaluation*

Data were processed using DataExplorer™ 4.9. Structural assignments were based on molecular weight identification, on the knowledge of the N-glycan biosynthesis and on MS/MS analysis of specific glycoforms, when possible. N-glycan species were identified by bioinformatics such as Expasy GlycoMod (http://web.expasy.org/glycomod/), Glycoworkbench v2.1 [64] and by the Consortium for Functional Glycomics glycan structures central database.

## 5. Conclusions

Our developed MS strategy led to a considerable improvement in upper mass range sensitivity and in signal-to-noise ratio, in addition to a significant increase in resolution of MALDI-TOF mass spectra, allowing a detailed mapping of human RBC N-glycans. Since RBCs have a relatively short lifespan, these analytical strategies could be used to study possible glycosylation changes that can occur during disease conditions, for the early detection of potential glyco-biomarkers. Most important, this developed strategy could be a useful tool to investigate the interaction mechanisms of pathogens recognition as well as the ABO(H) blood group mediated response to viral infections, with special regards to SARS-CoV-2.

**Supplementary Materials:** The following are available online at www.mdpi.com/xxx/s1, Figure S1: MALDI-TOF MS profile (low mass-range: m/z 1500-3250) of permethylated human erythrocyte N-glycans from blood group A. Figure S2: MALDI-TOF MS profile (middle mass-range: m/z 3250-5000) of permethylated human erythrocyte N-glycans from blood group A. Figure S3: MALDI-TOF

MS profile (high mass-range: m/z 5000-10000) of permethylated human erythrocyte N-glycans from blood group A. Figure S4: MALDI-TOF MS profile (low mass-range: m/z 1500-3250) of permethylated human erythrocyte N-glycans from blood group B. Figure S5: MALDI-TOF MS profile (middle mass-range: m/z 3250-5000) of permethylated human erythrocyte N-glycans from blood group B. Figure S6: MALDI-TOF MS profile (high mass-range: m/z 5000-10000) of permethylated human erythrocyte N-glycans from blood group B. Figure S7: MALDI-TOF MS profile (low mass-range: m/z 1500-3250) of permethylated human erythrocyte N-glycans from blood group AB. Figure S8: MALDI-TOF MS profile (middle mass-range: m/z 3250-5000) of permethylated human erythrocyte N-glycans from blood group AB. Figure S8: MALDI-TOF MS profile (middle mass-range: m/z 3250-5000) of permethylated human erythrocyte N-glycans from blood group AB. Figure S9: MALDI-TOF MS profile (high mass-range: m/z 5000-10000) of permethylated human erythrocyte N-glycans from blood group AB. Figure S10: MALDI-TOF MS profile (low mass-range: m/z 1500-3250) of permethylated human erythrocyte N-glycans from blood group O. Figure S11: MALDI-TOF MS profile (middle mass-range: m/z 3250-5000) of permethylated human erythrocyte N-glycans from blood group O. Figure S12: MALDI-TOF MS profile (high mass-range: m/z 5000-10000) of permethylated human erythrocyte N-glycans from blood group O.

**Author Contributions:** Conceptualization, D.G. and R.B.; Methodology, R.O.B, A.M and A.P.; Validation, R.O.B, A.M and A.P.; Formal Analysis, R.O.B, A.M and A.P.; Investigation, R.O.B, A.M and A.P.; Data Curation, R.O.B, A.M and A.P.; Writing – Original Draft Preparation, R.O.B, A.M and A.P.; Writing – Review & Editing, L.S.; Supervision, L.S, R.B. and D.G.

**Funding:** This research received no external funding.

**Institutional Review Board Statement:** The study was conducted according to the guidelines of the Declaration of Helsinki. Ethic committee approval was not required in our institution as the analyses performed in this study were carried out in the context of sampling for blood type analyses.

**Informed Consent Statement:** : Informed consent was obtained from all subjects involved in the study.

**Data Availability Statement:** All the MALDI TOF mass spectra and the MS/MS spectra recorded of permethylated N-glycans released by PNGase F can be downloaded from: www.ipcb.ct.cnr.it/ct/spectraVisualizza.jsp.

**Conflicts of Interest:** The authors declare no conflict of interest.

## References

1. Ji, P.; Murata-hori, M.; Lodish, H.F. Formation of mammalian erythrocytes: chromatin condensation and enucleation. *Trends Cell Biol.* **2011**, 21, 409–415; DOI:10.1016/j.tcb.2011.04.003.
2. Goodman, S.R.; Kurdia, A.; Ammann, L.; Kakhniashvili, D.; Daescu, O. The human red blood cell proteome and interactome. *Exp. Biol. Med.* **2007**, 232, 1391–1408; DOI: 10.3181/0706-MR-156.
3. Bryk, A.H.; Wiśniewski, J.R. Quantitative Analysis of Human Red Blood Cell Proteome. *J. Proteome Res.* **2017**, 16, 2752–2761; DOI: 10.1021/acs.jproteome.7b00025.
4. Phillips, D.R.; Morrison, M. The arrangement of Proteins in the human erythrocyte membrane. *Biochem. Biophys. Res. Commun.* **1970**, 40, 284–289; DOI: 10.1016/0006-291x(70)91007-7.
5. De Oliveira, S.; Saldanha, C. An overview about erythrocyte membrane. *Clin. Hemorheol. Microcirc.* **2010**, 44, 63–74; DOI: 10.3233/CH-2010-1253.
6. Delaunay, J. The molecular basis of hereditary red cell membrane disorders. *Blood Rev.* **2007**, 21, 1–20; DOI: 10.1016/j.blre.2006.03.005.
7. Hochmuth, R. Erythrocyte Membrane Elasticity And Viscosity. *Annu. Rev. Physiol.* **1987**, 49, 209–219; DOI: 10.1146/annurev.ph.49.030187.001233.
8. Varki, A. Biological roles of glycans. *Glycobiology* **2017**, 27, 3–49. DOI: 10.1093/glycob/cww086.
9. Stevens, J.; Blixt, O.; Tumpey, T.M.; Taubenberger, J.K.; Paulson, J.C.; Wilson, I.A. Structure and Receptor Specificity of the Hemagglutin from an H5N1 Influenza Virus. *Science* **2006**, 312, 404–410; DOI: 10.1126/science.1124513.
10. Pinho, S.S.; Reis, C.A. Glycosylation in cancer: Mechanisms and clinical implications. *Nat. Rev. Cancer* **2015**, 15, 540–555; DOI: 10.1038/nrc3982.
11. Magalhães, A.; Duarte, H.O.; Reis, C.A. Aberrant Glycosylation in Cancer: A Novel Molecular Mechanism Controlling Metastasis. *Cancer Cell* **2017**, 31, 733–735; DOI: 10.1016/j.ccell.2017.05.012.
12. Shade, K.T.C.; Anthony, R. Antibody Glycosylation and Inflammation. Antibodies **2013**, 2, 392–414; DOI: 10.3390/antib2030392.
13. Albrecht, S.; Unwin, L.; Muniyappa, M.; Rudd, P.M. Glycosylation as a marker for inflammatory arthritis. *Cancer Biomarkers* **2014**, 14, 17–28; DOI: 10.3233/CBM-130373.

14. Hwang, H.; Zhaang, J.; Chung, K.A.; Leverenz, J.B.; Zabetian, C.P.; Peskind, E.R.; Jankovic, J.; Su, Z.; Hancock, A.M.; Pan, C.; et al. Glycoproteomics in neurodegenerative diseases. *Mass Spectrom. Rev.* **2010**, 29, 79–125; DOI: 10.1002/mas.20221.
15. Palmigiano, A.; Barone, R.; Sturiale, L.; Sanfilippo, C.; Bua, R.O.; Romeo, D.A.; Messina, A.; Capuana, M.L.; Maci, T.; Le Pira, F.; et al. CSF N-glycoproteomics for early diagnosis in Alzheimer's disease. *J. Proteomics* **2016**, 131, 29–37; DOI: 10.1016/j.jprot.2015.10.006.
16. Jaeken, J. Congenital disorders of glycosylation. *Ann. N. Y. Acad. Sci.* **2010**, 1214, 190–198.
17. Barone, R.; Sturiale, L.; Garozzo, D. Mass spectrometry in the characterization of human genetic N-glycosylation defects. *Mass Spectrom. Rev.* **2009**, 28, 517–542; DOI: 10.1002/mas.20201.
18. Aoki, T. A Comprehensive Review of Our Current Understanding of Red Blood Cell (RBC) Glycoproteins. *Membranes* **2017**, 7, 1–19; DOI: 10.3390/membranes7040056.
19. Fukuda, M.; Dell, A.; Oates, J.E.; Fukuda, M.N. Structure of Branched Lactosaminoglycan, the Carbohydrate Moiety of Band 3 Isolated from Adult Human Erythrocytes. *J. Biol. Chem.* **1984**, 259, 8260–8273; DOI: 10.1016/S0021-9258(17)39722-3.
20. Tsuji, T.; Irimura, T.; Osawa, T. The carbohydrate moiety of band 3 glycoprotein of human erythrocyte membranes. Structures of lower molecular weight oligosaccharides. *J. Biol. Chem.* **1981**, 256, 10497–10502; DOI: 10.1016/S0021-9258(19)68649-7.
21. Yoshima, H.; Furthmayr, H.; Kobata, A. Structures of the asparagine-linked sugar chains of glycophorin A. *J. Biol. Chem.* **1980**, 255, 9713–9718; DOI: 10.1016/S0021-9258(18)43451-5.
22. Irimura, T.; Tsuji, T.; Tagami, S.; Yamamoto, K.; Osawa, T. Structure of a Complex-Type Sugar Chain of Human Glycophorin A. *Biochemistry* **1981**, 20, 560–566; DOI: 10.1021/bi00506a018.
23. Wilczynska, Z.; Miller-Podraza, H.; Koscielak, J. The contribution of different glycoconjugates to the total ABH blood group activity of human erythrocytes. *FEBS Lett.* **1980**, 112, 277–279; DOI: 10.1016/0014-5793(80)80197-9.
24. Krusius, T.; Finne, J.; Rauvala, H. The Poly(glycosy1) Chains of Glycoproteins. Characterisation of a novel type of glycoprotein saccharides from human erythrocyte membrane. *Eur. J. Biochem.* **1978**, 92, 289–300; DOI: 10.1111/j.1432-1033.1978.tb12747.x.
25. Fredriksson, S.Å.; Podbielska, M.; Nilsson, B.; Lisowska, E.; Krotkiewski, H. ABH blood group antigens in N-glycan of human glycophorin A. *Arch. Biochem. Biophys.* **2010**, 498, 127–135; DOI: 10.1016/j.abb.2010.04.017.
26. Lee-Sundlov, M.M.; Stowell, S.R.; Hoffmeister, K.M. Multifaceted role of glycosylation in transfusion medicine, platelets, and red blood cells. *J. Thromb. Haemost.* **2020**, 18, 1535–1547; DOI: 10.1111/jth.14874.
27. Stowell, S.R.; Stowell, C.P. Biologic roles of the ABH and Lewis histo-blood group antigens part II: thrombosis, cardiovascular disease and metabolism. *Vox Sang.* **2019**, 114, 535–552; DOI: 10.1111/vox.12786.
28. Siransy, L.K.; Nanga, Z.Y.; Zaba, F.S.; Tufa, N.Y.; Dasse, S.R. ABO/Rh Blood Groups and Risk of HIV Infection and Hepatitis B among Blood Donors of Abidjan, Côte D'Ivoire. *Eur. J. Microbiol. Immunol.* **2015**, 5, 205–209; DOI: 10.1556/1886.2015.00029.
29. Degarege, A.; Gebrezgi, M.T.; Ibanez, G.; Wahlgren, M.; Madhivanan, P. Effect of the ABO blood group on susceptibility to severe malaria: A systematic review and meta-analysis. *Blood Rev.* **2019**, 33, 53–62; DOI: 10.1016/j.blre.2018.07.002.
30. Horby, P.; Nguyen, N.Y.; Dunstan, S.J.; Baillie, J.K. The role of host genetics in susceptibility to influenza: A systematic review. *PLoS One* **2012**, 7, 1–9. DOI: 10.1371/journal.pone.0033180.
31. Li, D.; Wang, M.; Qi, J.; Zhang, Q.; Wang, H.; Pang, L.; Sun, X.; Duan, Z. Human group A rotavirus P[25] VP8* specifically binds to A-type histo-blood group antigen. *Virology* **2021**, 555, 56–63; DOI: 10.1016/j.virol.2020.12.016.
32. Tyrrell, D.; P, S.; AS, B. Relation between Blood Groups and Resistance to Infection with Influenza and some Picornaviruses. *Nature* **1968**, 220, 819–820; DOI: 10.1038/220819a0.
33. Davison, G.M.; Hendrickse, H.L.; Matsha, T.E. Membrane Influence Human Immunodeficiency Virus Infection? *Cells* **2020**, 845, 1–11; DOI: 10.3390/cells9040845.
34. Wu, Y.; Feng, Z.; Li, P.; Yu, Q. Relationship between ABO blood group distribution and clinical characteristics in patients with COVID-19. *Clin. Chim. Acta* **2020**, 509, 220–223; DOI: 10.1016/j.cca.2020.06.026.
35. e Fernandes, T.d.S. Chaotic model for COVID-19 growth factor. *Res. Biomed. Eng.* **2020**, 1–5; DOI: 10.1007/s42600-020-00077-5.
36. Liu, Y.; Häussinger, L.; Steinacker, J.M.; Dinse-Lambracht, A. Association between the dynamics of the COVID-19 epidemic and ABO blood type distribution. *Epidemiol. Infect.* **2021**, 149, 1–6; DOI: 10.1017/S0950268821000030.
37. Pendu, J. Le; Breiman, A.; Rocher, J.; Dion, M.; Ruvoën-Clouet, N. ABO Blood Types and COVID-19: Spurious, Anecdotal, or Truly Important Relationships? A Reasoned Review of Available Data. *Viruses* **2021**, 13, 1–21; DOI: 10.3390/v13020160.
38. Harvey, D.J. Proteomic analysis of glycosylation: Structural determination of N- and O-linked glycans by mass spectrometry. *Expert Rev. Proteomics* **2005**, 2, 87–101; DOI: 10.1586/14789450.2.1.87.
39. Banazadeh, A.; Veillon, L.; Wooding, K.M.; Zabet, M. Recent Advances in Mass Spectrometric Analysis of Glycoproteins. *Electrophoresis.* **2017**, 38, 162–189; DOI: 10.1002/elps.201600357.
40. North, S.J.; Gunten, S. von; Antonopoulos, A.; Trollope, A.; Jr, D.W.M.; Jang-lee, J.; Dell, A.; Metcalfe, D.D.; Kirshenbaum, A.S.; Bochner, B.S.; et al. Glycomic analysis of human mast cells, eosinophils and basophils. *Glycobiology* **2012**, 22, 12–22; DOI: 10.1093/glycob/cwr089.
41. Walther, T.; Karamanska, R.; Chan, R.W.Y.; Chan, M.C.W.; Jia, N.; Air, G.; Hopton, C.; Wong, M.P.; Dell, A.; Malik Peiris, J.S.; et al. Glycomic Analysis of Human Respiratory Tract Tissues and Correlation with Influenza Virus Infection. *PLoS Pathog.* **2013**, 9; DOI: 10.1371/journal.ppat.1003223.
42. Vreeker, G.C.M.; Bladergroen, M.R.; Nicolardi, S.; Mesker, W.E.; Tollenaar, R.A.E.M.; van der Burgt, Y.E.M.; Wuhrer, M. Dried blood spot N-glycome analysis by MALDI mass spectrometry. *Talanta* **2019**, 205, 120104; DOI: 10.1016/j.talanta.2019.06.104.

43. Fukuda, M.N.; Dell, A.; Scartezzinill, P. Primary Defect of Congenital Dyserythropoietic Anemia Type II. Failure in glycosylation of erythrocyte lactosaminoglycan proteins caused by lowered N-acetylglucosaminyltransferase II. *J. Biol. Chem.* **1987**, 262, 7195–7206; DOI: 10.1016/S0021-9258(18)48223-3.
44. Denecke, J.; Kranz, C.; Nimtz, M.; Conradt, H.S.; Brune, T.; Heimpel, H.; Marquardt, T. Characterization of the N-glycosylation phenotype of erythrocyte membrane proteins in congenital dyserythropoietic anemia type II (CDA II / HEMPAS). *Glycoconj. J.* **2008**, 25, 375–382; DOI: 10.1007/s10719-007-9089-1.
45. Domon, B.; Costello, C.E. A systematic nomenclature for carbohydrate fragmentations in FAB-MS/MS spectra of glycoconjugates. *Glycoconj. J.* **1988**, 5, 397–409; DOI: 10.1007/BF01049915.
46. Daniels, G. ABO, H, and Lewis Systems. In Human Blood Groups; 2013; pp. 11–95, Print ISBN: 9781444333244.
47. Pisano, A.; Redmond, J.W.; Williams, K.L.; Gooley, A.A. Glycosylation sites identified by solid-phase edman degradation: O-linked glycosylation motifs on human glycophorin A. *Glycobiology* **1993**, 3, 429–435; DOI: 10.1093/glycob/3.5.429.
48. Zdebska, E.; Kościelak, J. A single-sample method for determination of carbohydrate and protein contents glycoprotein bands separated by sodium dodecyl sulfate-polyacrylamide gel electrophoresis. *Anal. Biochem.* **1999**, 275, 171–179; DOI: 10.1006/abio.1999.4294.
49. Climer, L.K.; Dobretsov, M.; Lupashin, V. Defects in the COG complex and COG-related trafficking regulators affect neuronal Golgi function. *Front. Neurosci.* **2015**, 9, 1–9; DOI: 10.3389/fnins.2015.00405.
50. Palmigiano, A.; Bua, R.O.; Barone, R.; Rymen, D.; Régal, L.; Deconinck, N.; Dionisi-Vici, C.; Fung, C.W.; Garozzo, D.; Jaeken, J. and Sturiale, L. MALDI-MS profiling of serum O-glycosylation and N-glycosylation in COG5-CDG. *J. Mass Spectrom.* **2017**, 52, 372–377; DOI: 10.1002/jms.3936.
51. Fukuda, M.N.; Masri, K.A.; Dell, A.; Thonar, E.J.; Klier, G. and Lowenthal, R.M. Defective glycosylation of erythrocyte membrane glycoconjugates in a level of membrane-bound form of galactosyltransferase. *Blood* **1989**, 73, 1331–1339; DOI: 10.1182/blood.V73.5.1331.1331Get.
52. Samanta, S.; Dutta, D.; Ghoshal, A.; Mukhopadhyay, S.; Saha, B.; Sundar, S.; Jarmalavicius, S.; Forgber, M.; Mandal, C.; Walden, P.; et al. Glycosylation of erythrocyte spectrin and its modification in visceral leishmaniasis. *PLoS One* **2011**, 6; DOI: 10.1371/journal.pone.0028169.
53. Gamblin, S. J.; Haire, L. F.; Russell, R. J.; Stevens, D. J.; Xiao, B.; Ha, Y.; Vasisht, N.; Steinhauer, D. A.; Daniels, R. S.; Elliot, A.; Wiley, D.C. and Shekel, J.J. The Structure and Receptor Binding Properties of the 1918 Influenza Hemagglutinin. *Science* **2004**, 303, 1838–1842; DOI: 10.1126/science.1093155.
54. Aich, U.; Beckley, N.; Shriver, Z.; Raman, R.; Viswanathan, K. Glycomics-based analysis of chicken red blood cells provides insight into the selectivity of the viral agglutination assay. *FEBS J.* **2011**, 278, 1699–1712; DOI: 10.1111/j.1742-4658.2011.08096.x.
55. Klimov, A.; Balish, A.; Veguilla, V.; Sun, H.; Schiffer, J.; Lu, X.; Katz, J.M.; Hancock, and K. Influenza Virus Titration, Antigenic Characterization, and Serological Methods for Antibody Detection. In Influenza Virus: Methods and Protocols; Press, H., Ed.; 2012; Vol. 1, pp. 25–51 ISBN 978-1-61779-620-3.
56. Nobusawa, E.; Ishihara, H.; Morishita, T.; Sato, K.; Nakajima, K. Change in receptor-binding specificity of recent human influenza A viruses (H3N2): A single amino acid change in hemagglutinin altered its recognition of sialyloligosaccharides. *Virology* **2000**, 278, 587–596; DOI: 10.1006/viro.2000.0679.
57. Bull, P.C.; Lowe, B.S.; Kortok, M.; Molyneux, C.S.; Newbold, C.I.; Marsh,K. Parasite antigens on the infected red cell surface are targets for naturally acquired immunity to malaria. *Nat. Med.* **1998**, 4, 358–360; DOI: 10.1038/nm0398-358.
58. Katz, J.M.; Hancock, K.; Xu, X. Serologic assays for influenza surveillance, diagnosis and vaccine evaluation. *Expert Rev. Anti. Infect. Ther.* **2011**, 9, 669–683; DOI: 10.1586/eri.11.51.
59. Chandrasekaran, A.; Srinivasan, A.; Raman, R.; Viswanathan, K.; Raguram, S.; Tumpey, T.M.; Sasisekharan, V.; Sasisekharan, R. Glycan topology determines human adaptation of avian H5N1 virus hemagglutinin. *Nat. Biotechnol.* **2008**, 26, 107–113; DOI: 10.1038/nbt1375.
60. Srinivasan, A.; Viswanathan, K.; Raman, R.; Chandrasekaran, A.; Raguram, S.; Tumpey, T.M.; Sasisekharan, V.; Sasisekharan, R. Quantitative biochemical rationale for differences in transmissibility of 1918 pandemic influenza A viruses. *PNAS.* **2008**, 15, 2800–2805; DOI: 10.1073/pnas.0711963105.
61. Dodge, T.; Hanahan, J. The Preparation and Chemical Characteristics Erythrocytes of Hemoglobin-Free Ghosts of Human Erythrocytes. *Arch. Biochem. Biophys.* **1963**, 100, 119–130; DOI: 10.1016/0003-9861(63)90042-0.
62. Palmigiano, A.; Messina, A.; Bua, R.O.; Barone, R.; Sturiale, L.; Zappia, M.; Garozzo, D. CSF N-Glycomics Using MALDI MS Techniques in Alzheimer's Disease. In Biomarkers Alzheimer's Dis. Drug Dev. 2018, 1750, 75-91 Humana Press, New York, NY.
63. Sturiale, L.; Barone, R.; Garozzo, D. The impact of mass spectrometry in the diagnosis of congenital disorders of glycosylation. *J. Inherit. Metab. Dis.* **2011**, 34, 891–899; DOI: 10.1007/s10545-011-9306-8.
64. Ceroni, A.; Maass, K.; Geyer, H.; Geyer, R.; Dell, A.; Haslam, S.M. GlycoWorkbench: A tool for the computer-assisted annotation of mass spectra of glycans. *J. Proteome Res.* **2008**, 7, 1650–1659; DOI: 10.1021/pr7008252.